

On the Impact of Oscillator Phase Noise in an IRS-assisted MISO TDD System

Chu Li, Aydin Sezgin
Ruhr-Universität Bochum, Germany
Email: {chu.li, aydin.sezgin}@rub.de

Zhu Han
University of Houston, USA
zhan2@uh.edu

Abstract—Intelligent reflecting surfaces (IRS) have great potential for achieving higher spectral and energy efficiency. However, the expected benefits depend strongly on the accuracy of the channel estimation. Most of the current work assumes perfect channel state information, which is impractical in real communication systems. Moreover, state-of-the-art IRS channel estimation algorithms are proposed under the assumption of perfect transceivers. These algorithms cannot be applied in the case of imperfect transceivers. In this work, we propose a novel channel estimation algorithm that takes into account phase noise from the local oscillator, which is the major contributor to the transceiver impairments. More specifically, we estimate the channel from uplink pilots transmission. Utilizing the obtained channel estimates the downlink ergodic rate is analyzed, where we find that the IRS-assisted system becomes more robust to phase noise as the number of reflective elements increases. Additionally, the impact of additive receiver noise in uplink vanishes when the number of reflective elements approaches infinity.

Index Terms—Intelligent reflecting surfaces (IRS), phase noise, communication rate

I. INTRODUCTION

Intelligent reflection surface (IRS) aided wireless communication systems, as a promising technology to improve the spectral and energy efficiency for 5G and beyond networks, has received increasing attention. An IRS is a thin metal plate consisting of passive scattering elements that can be controlled by a low-cost electronic circuit. Recent works have proven that IRS-assisted systems can achieve higher spectral and energy efficiency at a lower cost than other technologies, such as conventional multi-input multi-output (MIMO) and relay-aided systems [1]–[3].

However, most prior works assume perfect knowledge of channel state information (CSI), which is highly unlikely given in practice. Especially for IRS-aided systems, obtaining accurate CSI is challenging. Unlike conventional transmitters and receivers that can transmit or receive pilot signals, IRS does not have radio resources or signal processing capabilities to estimate the channel. To address this issue, recent works estimate the cascaded channel instead of estimating the BS to IRS channel and the IRS to user channel separately [4] [5]. More specifically, in [4] the least-square (LS) based channel estimation is proposed, while a minimum mean square

mean square error (MMSE) based algorithm is applied in [5]. However, these works assume perfect transceivers. Yet, in practical systems phase noise from the local oscillator, which is the main contributor to transceiver impairments, has a detrimental effect on system performance. In particular, high-frequency oscillators suffer from strong phase noise [6]. Therefore, systems operating in the high-frequency range, such as terahertz (THz), are severely impacted by phase noise [7], [8]. The impact of additive phase noise in an IRS-assisted system is studied in [9]. In addition to the additive phase noise, the transceiver also suffers from multiplicative phase noise. Compared to additive phase noise, it can cause more severe degradation of system performance [10], [11]. Yet, the impact of the multiplicative phase noise has not been studied in an IRS-assisted system.

To fill this gap in research, in this work, we study the impact of the multiplicative phase noise in an IRS-assisted system. We consider an IRS-assisted system with multiplicative phase noise both at the BS and user. A novel channel estimation algorithm is proposed considering the phase noise. Particularly, we assume that the system operates in time division duplex (TDD) mode, the channel estimates are obtained from uplink pilots transmission. Exploiting the channel reciprocity we investigate the system performance in the downlink, more specifically, we derive the ergodic communication rate in closed form. Simulation results verify the correctness of the closed-form expression. We observe that the system becomes more robust against the phase noise as the number of reflective elements increases. Moreover, the influence of the additive receiver noise in uplink vanishes as the number of reflecting elements grows asymptotically large.

The rest of this paper is organized as follows. Sec. II describes the system model. In Sec. III we propose the channel estimation algorithm and analyze the downlink rate. Simulation results are provided in Sec. IV. Finally, Sec. V concludes the paper.

Notation : Boldface lower and upper case symbols are used to denote the vectors and matrices, respectively. $(\cdot)^T$, $(\cdot)^*$ and $(\cdot)^H$ represent the transpose, conjugate and Hermitian transpose operators. We use $\mathbb{E}[\cdot]$ to denote the expectation operator, $\text{diag}(\mathbf{a})$ is a diagonal matrix with vector \mathbf{a} on its main diagonal, and \mathbf{I}_N is a $N \times N$ identity matrix. $\text{tr}(\mathbf{X})$, $\|\mathbf{X}\|$ and $\text{vec}(\mathbf{X})$ denote the trace, norm and vectorization with respect to the matrix \mathbf{X} . \otimes is the Kronecker product.

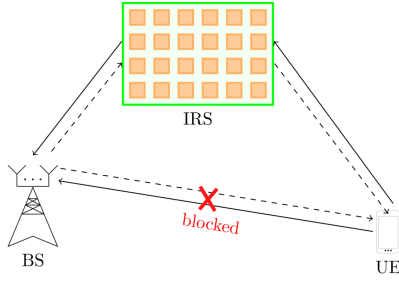


Fig. 1: IRS-assisted single user system: downlink channel (dashed lines) and uplink channel (solid lines)

II. SYSTEM MODEL

We consider a multiple-input single-output (MISO) system in which a BS with M antennas communicates with a user with a single antenna by means of an IRS composed of N reflective elements, as illustrated in Fig. 1. The phase shift induced by the IRS is controlled by a micro-controller connected to the BS. In addition, we assume that the channel between the BS and the user is blocked by obstacles, which is mostly the case in practice [12]. In this work, a block-fading channel is assumed. We use T to denote the channel coherence time. Furthermore, the communication system operates in TDD mode. We use $[\tau_1, \dots, \tau_B] \in T$ and $\mathcal{D} \triangleq \{1, \dots, T\} \setminus \{\tau_1, \dots, \tau_B\}$ to denote the time indices for uplink pilots and downlink data transmission, respectively. The received signal at the user is modeled as

$$\begin{aligned} y_t^{\text{dl}} &= (\mathbf{D}_t \mathbf{H}_1 \text{diag}(\phi_t^{\text{dl}}) \mathbf{h}_2)^T \mathbf{w}_t \varsigma_t + n_t^{\text{dl}} \\ &= (\mathbf{D}_t \mathbf{H}_{\text{cas}} \phi_t^{\text{dl}})^T \mathbf{w}_t \varsigma_t + n_t^{\text{dl}}, \quad t \in \mathcal{D}, \end{aligned} \quad (1)$$

where $\mathbf{D}_t = \text{diag}(e^{j\theta_{t,1}}, e^{j\theta_{t,2}}, \dots, e^{j\theta_{t,M}})$ denotes the multiplicative phase-drifts caused by the imperfect local oscillators at BS and user. Also, $\theta_{t,m} = \theta_{t,m}^{\text{BS}} + \theta_t^{\text{UE}}$, where $\theta_{t,m}^{\text{BS}}$ and θ_t^{UE} are, respectively, the phase-drifts at the m -th BS antenna and the user. Furthermore, $\theta_{t,m}^{\text{BS}}$ and θ_t^{UE} are modeled as a discrete-time independent Wiener process [11]

$$\theta_{t,m}^{\text{BS}} = \theta_{t-1,m}^{\text{BS}} + \Delta\theta_{t,m}^{\text{BS}}, \quad (2)$$

$$\theta_t^{\text{UE}} = \theta_{t-1}^{\text{UE}} + \Delta\theta_t^{\text{UE}}, \quad (3)$$

where $\Delta\theta_{t,m}^{\text{BS}} \sim \mathcal{N}(0, \sigma_{BS,m}^2)$ and $\Delta\theta_t^{\text{UE}} \sim \mathcal{N}(0, \sigma_{UE}^2)$ denote the random phase increment caused by the imperfect local oscillator at the BS and user, respectively. We assume that each antenna of the BS has its own local oscillator. Besides, we let $\sigma_{BS,m}^2 = \sigma_{BS}^2$ for each oscillator for simplicity. The phase noise variance is given by $\sigma_{BS/UE}^2 = 4\pi^2 f_c^2 T_s \zeta_{BS/UE}$, where f_c , T_s , $\zeta_{BS/UE}$ are the carrier frequency, the symbol interval and a constant that depends on the quality of the local oscillator, respectively. In addition, $\mathbf{H}_{\text{cas}} \in \mathbb{C}^{M \times N}$ represents the IRS-assisted channel given as $\mathbf{H}_{\text{cas}} = \mathbf{H}_1 \text{diag}(\mathbf{h}_2)$, where $\mathbf{H}_1 \in \mathbb{C}^{M \times N}$ and $\mathbf{h}_2 \in \mathbb{C}^N$ denote the BS to IRS and IRS to user channel, respectively. We model the entries of \mathbf{H}_{cas} as independent and identically distributed complex circularly symmetric Gaussian variables with variance β_{cas} . Moreover, we use $\phi_t^{\text{dl}} \in \mathbb{C}^N$ to denote the phase shifts vector at the IRS during the downlink transmission at time t , and

$\mathbf{w}_t \in \mathbb{C}^M$ is the precoding vector designed according to the channel estimates, which will be introduced in the following section. $\varsigma_t \in \mathbb{C}$ is the transmit symbol with power constraint $\mathbb{E}[|\varsigma_t|^2] = P$, and $n_t^{\text{DL}} \sim \mathcal{CN}(0, \sigma_{\text{d}}^2)$ is the additive complex Gaussian noise in the downlink. Similarly, we model the received signal at the BS as

$$\mathbf{y}_t^{\text{ul}} = (\mathbf{D}_t \mathbf{H}_{\text{cas}} \phi_t^{\text{ul}}) x_t + \mathbf{n}_t^{\text{ul}}, \quad t \in [\tau_1, \dots, \tau_B], \quad (4)$$

where $\phi_t^{\text{ul}} \in \mathbb{C}^N$ denotes the phase shifts vector at the IRS during the uplink pilots transmission at time t , and x_t is the pilots signal with $\mathbb{E}[|x_t|^2] = 1$. Lastly, $\mathbf{n}_t^{\text{ul}} \sim \mathcal{CN}(0, \sigma_{\text{u}}^2 \mathbf{I}_M)$ is the additive receiver noise at the BS with covariance $\sigma_{\text{u}}^2 \mathbf{I}_M$.

III. CHANNEL ESTIMATION SCHEME AND DOWNLINK ANALYSIS

In this section, we introduce the MMSE channel estimation algorithm in Sec. III-A. The obtained channel estimate is utilized to analyze the downlink performance in Sec. III-B.

A. Channel Estimation

To study the impact of the phase noise on the system performance, we propose the MMSE based channel estimation algorithm, by which the channel and the phase noise are jointly estimated. Exploiting the channel reciprocity in the TDD mode, we obtain the downlink channel from the uplink pilots signal. Since the pilot transmission is corrupted by the random phase drifts caused by the imperfect local oscillator, the conventional IRS channel estimation algorithms in [4], [5], [13] cannot be applied. To solve this problem, we propose an MMSE channel estimator considering the phase noise in the following.

We rewrite the received signal at the BS (4) as

$$\begin{aligned} \mathbf{y}_t^{\text{ul}} &= ((\phi_t^{\text{ul}})^T \otimes \mathbf{I}_M) (\mathbf{I}_N \otimes \mathbf{D}_t) \mathbf{h} x_t + \mathbf{n}_t \\ &= ((\phi_t^{\text{ul}})^T \otimes \mathbf{I}_M) \tilde{\mathbf{h}}_t x_t + \mathbf{n}_t, \end{aligned} \quad (5)$$

where $\tilde{\mathbf{h}} = \text{vec}(\mathbf{H}_{\text{cas}})$ is a MN dimensional vector, and we define $\tilde{\mathbf{h}} = (\mathbf{I}_N \otimes \mathbf{D}_t) \mathbf{h}$ as the effective channel. Note that the real channel \mathbf{h} is constant with the coherence time, while the effective channel $\tilde{\mathbf{h}}$ is, in contrast, time variant due to the random phase noise. During the uplink pilots transmission, we design the IRS phase shifts vector $\phi_{\tau_i}^{\text{ul}}$ as the i -th row of a $B \times N$ DFT matrix Φ , which is shown to be the optimal design of the IRS during uplink channel estimation [4], [5], [13]. Next, we introduce the MMSE estimator of $\tilde{\mathbf{h}}_t$.

Lemma 1. Given the combined uplink pilots signal $\boldsymbol{\psi} \triangleq [\mathbf{y}_{\tau_1}^T \dots \mathbf{y}_{\tau_B}^T]^T \in \mathbb{C}^{BM}$, the MMSE channel estimate of the effective channel $\tilde{\mathbf{h}}_t$ is given by

$$\hat{\mathbf{h}}_t = \frac{\beta_{\text{cas}}}{N\beta_{\text{cas}} + \sigma_{\text{u}}^2} \left((\Phi^H \tilde{\mathbf{D}}) \otimes \mathbf{I}_M \right) \boldsymbol{\psi}, \quad (6)$$

where

$$\tilde{\mathbf{D}} = \text{diag} \left(x_{\tau_1}^* e^{-\frac{\sigma_{BS}^2 + \sigma_{UE}^2}{2} |t - \tau_1|}, \dots, x_{\tau_B}^* e^{-\frac{\sigma_{BS}^2 + \sigma_{UE}^2}{2} |t - \tau_B|} \right). \quad (7)$$

The corresponding covariance matrix of the channel estimates is given as

$$\begin{aligned}\Psi_t &= \mathbb{E} \left[\hat{\mathbf{h}}_t \hat{\mathbf{h}}_t^H \right] \\ &= \frac{\beta_{cas}^2}{N\beta_{cas} + \sigma_u^2} \left(\Phi^H \tilde{\mathbf{D}} \tilde{\mathbf{D}}^H \Phi \right) \otimes \mathbf{I}_M,\end{aligned}\quad (8)$$

while the estimation error covariance matrix is

$$\begin{aligned}\mathbf{C}_t &= \mathbb{E} \left[\left(\tilde{\mathbf{h}}_t - \hat{\mathbf{h}}_t \right) \left(\tilde{\mathbf{h}}_t - \hat{\mathbf{h}}_t \right)^H \right] \\ &= \beta_{cas} \mathbf{I}_{MN} - \frac{\beta_{cas}^2}{N\beta_{cas} + \sigma_u^2} \left(\Phi^H \tilde{\mathbf{D}} \tilde{\mathbf{D}}^H \Phi \right) \otimes \mathbf{I}_M.\end{aligned}\quad (9)$$

Proof. The proof is provided in Appendix A. \square

B. Downlink Performance Analysis

Utilizing the channel estimates proposed in Sec. III-A, we investigate the impact of the phase noise on the downlink performance. According to (1), we define the received instantaneous SNR as

$$\gamma_t = \frac{P}{\sigma_d^2} \left| \left(\mathbf{D}_t \mathbf{H}_{cas} \phi_t^{dl} \right)^T \mathbf{w}_t \right|^2, \quad (10)$$

where the precoding vector \mathbf{w}_t depends on the channel estimates. More specifically, we design the precoding vector under maximum ratio transmission (MRT), which is given as

$$\mathbf{w}_t = \frac{\left(\hat{\mathbf{H}}_{cas,t} \phi_t^{dl} \right)^*}{\left(\mathbf{E} \left[\left\| \hat{\mathbf{H}}_{cas,t} \phi_t^{dl} \right\|^2 \right] \right)^{\frac{1}{2}}}. \quad (11)$$

Here, we normalize the precoding vector over the average of many channel realizations for analytical tractability. Next, we optimize the IRS by maximizing the received SNR given in (10). Thus, the optimal IRS is given as [5], [13]

$$\phi_{t,opt}^{DL} = \exp \left(j \angle \left(\hat{\mathbf{H}}_{cas,t}^H \mathbf{1}_N \right) \right). \quad (12)$$

Plugging (11) and (12) into (10), the instantaneous SNR can be observed under the optimized IRS. We now define the ergodic communication rate as

$$R = \frac{1}{T} \sum_{t \in D} \log_2 (1 + \mathbb{E} [\gamma_t]). \quad (13)$$

We notice that the ergodic rate depends on the averaged SNR $\mathbb{E} [\gamma_t]$, which can be naively computed by taking the average over many instantaneous SNR. However, it leads to high computational complexity, particularly when the communication system has a large number of antennas at the BS or reflective elements at the IRS. To overcome this issue, we present the averaged SNR in a closed-form in the following theorem.

Theorem 1. Given the MMSE channel estimates proposed in Sec. III-B, the averaged SNR with random IRS is given by

$$\bar{\gamma}_{t,a} = \frac{P}{\sigma_d^2} \left((M-1) N \eta + N \beta_{cas} \right), \quad (14)$$

while the averaged SNR with optimized IRS is given by

$$\bar{\gamma}_{t,opt} = \frac{P}{\sigma_d^2} \left(\left((M-1) + \frac{N\pi}{4} - 1 \right) N \eta + N \beta_{cas} \right), \quad (15)$$

where $\eta = \frac{(\beta_{cas})^2}{N\beta_{cas} + \sigma_u^2} \sum_{i=1}^N e^{-(\sigma_{BS}^2 + \sigma_{UE}^2)(t-i)}$.

Proof. The proof is provided in Appendix B. \square

It is easy to see that under perfect CSI, i.e., $\sigma_{BS}^2 = \sigma_{UE}^2 = 0$ and $\sigma_u^2 = 0$, η in (14) and (15) is equivalent to the channel gain β_{cas} . Thus, we use η to denote the gain of the channel estimates. Furthermore, we have $\eta \xrightarrow[N \rightarrow \infty]{a.s.} \frac{\beta_{cas}}{N} \sum_{i=1}^N e^{-(\sigma_{BS}^2 + \sigma_{UE}^2)(t-i)}$, which shows that the impact of the additive noise during channel estimation with variance σ_u^2 gradually vanishes as $N \rightarrow \infty$. Meanwhile, we observe that η is increasing with N , implying that the system can tolerate stronger phase noise as N increases. The proof is omitted due to lack of space. Finally, by substituting (14) and (15) to (13) we observe the ergodic communication rate with random and optimized IRS, respectively.

Remark 1. Note that the entries of the channel estimates $\hat{\mathbf{h}}_t$ in Lemma 1 are correlated due to the phase noise, since Ψ_t in (8) is not a diagonal matrix. However, the variance of the phase noise σ_{BS}^2 and σ_{UE}^2 is usually small in practice, which makes the entries on the main diagonal of Ψ_t dominant compared to the other entries. Therefore, for simplicity, we ignore the correlation of the channel estimates in this work. We consider Theorem 1 as a reasonable lower bound for the averaged SNR, while an exact analysis considering the correlation will be introduced in our future work.

IV. SIMULATION RESULTS

In this section, the system performance in terms of ergodic rate is presented when the proposed channel estimates are applied for downlink data transmission. More specifically, we study how the additive noise during uplink channel estimation and the multiplicative phase noise affect the system performance.

Throughout the simulation, we set the center frequency $f_c = 2.5$ GHz, the symbol time interval $T_s = 10^{-7}$ s. Additionally, the number of the BS antennas is set to 16, and the length of the coherence block is $T = 500$. Furthermore, we assume a transmit power $P = 30$ dBm and a noise variance $\sigma_d^2 = -80$ dBm. The path loss parameter of β_{cas} is modeled as $\beta_{cas} = C_0 \left(\frac{d_{cas}}{D_0} \right)^{-\alpha}$, where we set the reference path loss $C_0 = -30$ dB, the path distance $d_{cas} = 100$ m, and the path loss factor α to 2. The markers in the following figures are the theoretical results according to Theorem 1, while the curves are the simulation results. As described in Remark 1, we also ignore the correlation between the channel estimates in our simulations. We simulate the channel estimate $\hat{\mathbf{h}}$ that follows complex Gaussian distribution with covariance $\eta \mathbf{I}_{MN}$.

We first investigate the impact of the additive noise during the uplink under the assumption of perfect hardware. Fig. 2 (a) plots the ergodic rate with random (Rand.) and optimized (Opt.) IRS utilizing the proposed MMSE channel estimates.

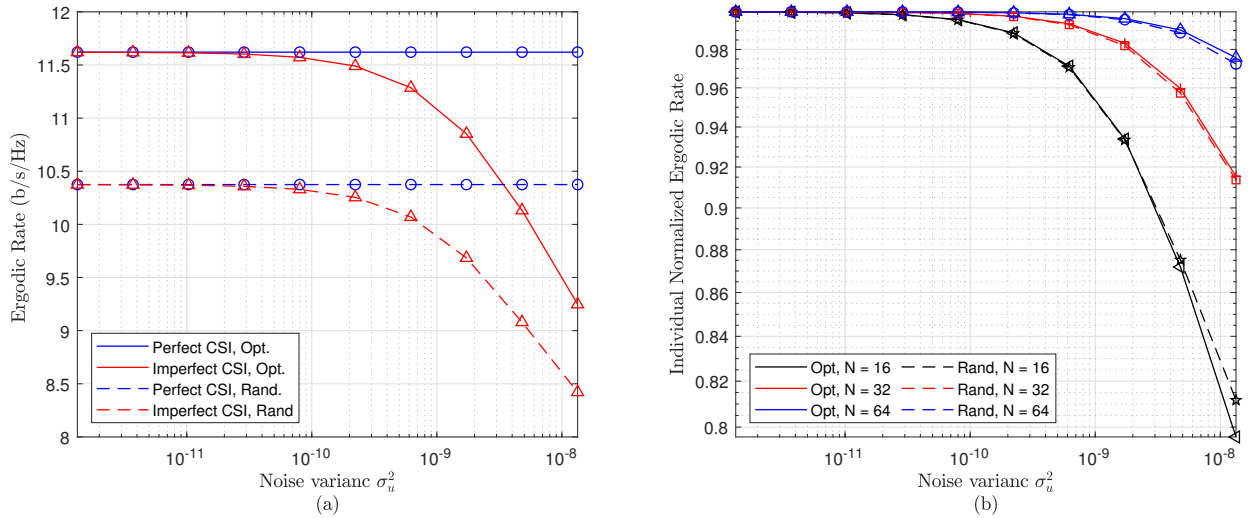


Fig. 2: Performance comparison between random and optimized IRS against noise variance σ_u^2 for $M = 16$, $\zeta_{BS} = \zeta_{UE} = 0$, (a) Ergodic rate with optimized and random IRS for $N = 16$, (b) Individual normalized ergodic rate with optimized and random IRS

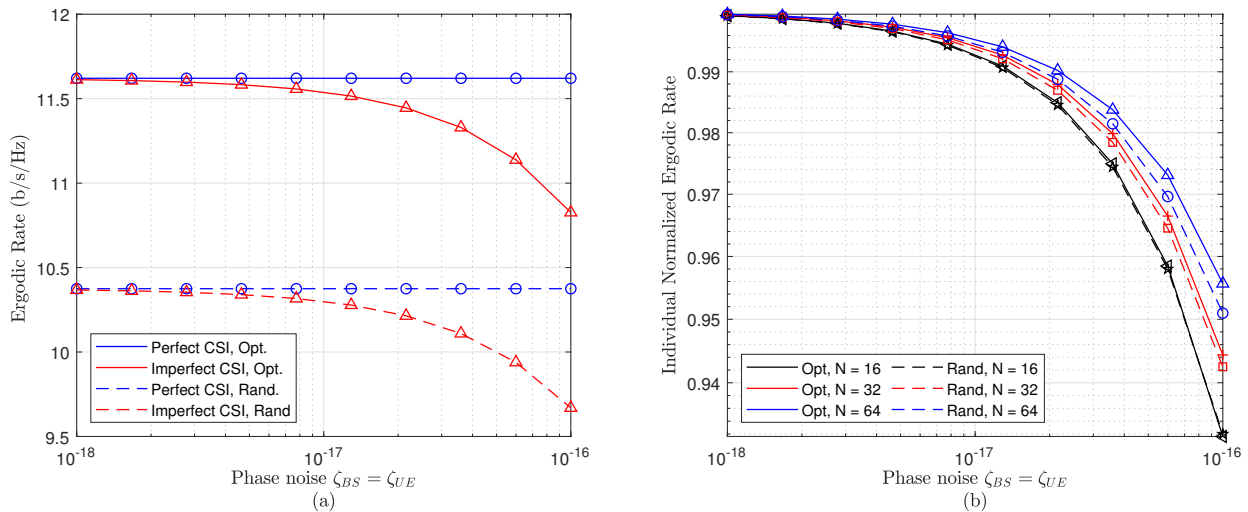


Fig. 3: Performance comparison between random and optimized IRS against the phase noise parameter ζ_{BS} and ζ_{UE} for $M = 16$, $\frac{\beta_{oas}}{\sigma_u^2} = 20$ dB, (a) Ergodic rate with optimized and random IRS for $N = 16$, (b) Individual normalized ergodic rate with optimized and random IRS

Meanwhile, the ergodic rate under the MMSE channel estimates and perfect CSI are compared. We notice that the simulation results agree perfectly with the analytical expressions. Furthermore, the ergodic rate decreases with increasing σ_u^2 . This is because σ_u^2 affects the gain of the channel estimates η as introduced in Sec. III-B. We also find that the system with optimized IRS performs better than that with random IRS. To study the influence of the number of reflective elements N on system performance, we plot the individual normalized ergodic rate in Fig. 2 (b), which is computed by dividing the ergodic rate under MMSE estimate by it under perfect CSI. It can be clearly seen that the impact of noise becomes weaker as N increases for both random and optimized IRS.

An interesting observation is that the system with random IRS is slightly more robust to the additive noise when N is small, i.e. $N = 16$, while as N increases, the system with optimized IRS becomes more robust than with random IRS.

Next, we study the effects of phase noise on the ergodic communication rate. In Fig. 3 (a), we compare the ergodic rate of the optimized and random IRS with respect to the phase noise parameter. It can be seen that the communication rate under imperfect CSI approaches the rate of the perfect CSI as the phase noise becomes smaller. Furthermore, we find that the system with optimized IRS still outperforms the system with random IRS when phase noise is taken into account. The individual normalized ergodic rate as a function of the phase

noise parameter is shown in Fig. 3 (b), from which we see that the impact of phase noise decreases with increasing N . Moreover, with increasing N , the robustness of the system with optimized IRS to phase noise becomes higher than that of the system with random IRS.

V. CONCLUSION

In this work, we have investigated the effects of phase noise in an IRS-assisted MISO communication system. We proposed a MMSE-based channel estimation algorithm that takes into account the phase noise caused by the imperfect local oscillator. Using the proposed MMSE estimates, we studied the ergodic downlink rate numerically and analytically, where we find that the robustness to the phase noise increases as the number of reflecting elements increases. We have also shown that the influence of additive noise during uplink channel estimation vanishes as N approaches infinity.

APPENDIX

A. Proof of Lemma 1

According to [14] the MMSE estimator of the effective channel is given by

$$\hat{\mathbf{h}}_t = \mathbb{E} \left[\tilde{\mathbf{h}}_t \psi^H \right] \left(\mathbb{E} [\psi \psi^H] \right)^{-1} \psi. \quad (16)$$

where the first term is

$$\begin{aligned} & \mathbb{E} \left[\tilde{\mathbf{h}}_t \psi^H \right] \\ & \stackrel{(a)}{=} \mathbb{E} \left[(\mathbf{I}_N \otimes \mathbf{D}_t) \mathbf{h} \mathbf{h}^H (\Phi^H \otimes \mathbf{I}_M) \right. \\ & \quad \left. \text{diag} [x_{\tau_1}^* \mathbf{D}_{\tau_1}^H, \dots, x_{\tau_B}^* \mathbf{D}_{\tau_B}^H] \right] \\ & = \beta_{cas} \mathbf{I}_{MN} \mathbb{E} \left\{ (\Phi^H \otimes \mathbf{I}_M) \right. \\ & \quad \left. \text{diag} [x_{\tau_1}^* \mathbf{D}_{\tau_1}^H, \dots, x_{\tau_B}^* \mathbf{D}_{\tau_B}^H] \right\} \\ & \stackrel{(b)}{=} \beta_{cas} \mathbf{I}_{MN} (\Phi^H \otimes \mathbf{I}_M) \text{diag} \left[x_{\tau_1}^* e^{-\frac{\sigma_{BS}^2 + \sigma_{UE}^2}{2} |t - \tau_1|} \mathbf{I}_M \right. \\ & \quad \left. \dots, x_{\tau_B}^* e^{-\frac{\sigma_{BS}^2 + \sigma_{UE}^2}{2} |t - \tau_B|} \mathbf{I}_M \right] \\ & = (\beta_{cas} \Phi^H \tilde{\mathbf{D}}) \otimes \mathbf{I}_M, \end{aligned} \quad (17)$$

in which (a) exploits the fact that the additive noise is uncorrelated with the channel \mathbf{h} , and (b) utilizes $\mathbb{E} [e^{j\theta_{t1,m}} e^{j\theta_{t2,m}}] = e^{-\frac{\sigma_{BS}^2 + \sigma_{UE}^2}{2} |t1 - t2|}$. $\tilde{\mathbf{D}}$ in (17) is given in (7). Furthermore, we have

$$\begin{aligned} & \mathbb{E} [\psi \psi^H] \\ & = \mathbb{E} \left\{ \text{diag} [x_{\tau_1} \mathbf{D}_{\tau_1}, \dots, x_{\tau_B} \mathbf{D}_{\tau_B}] (\Phi \otimes \mathbf{I}_M) \mathbf{h} \mathbf{h}^H \right. \\ & \quad \left. (\Phi^H \otimes \mathbf{I}_M) \text{diag} [x_{\tau_1}^* \mathbf{D}_{\tau_1}^H, \dots, x_{\tau_B}^* \mathbf{D}_{\tau_B}^H] \right\} + \sigma_u^2 \mathbf{I}_{MB} \\ & \stackrel{(a)}{=} \Omega \otimes \mathbf{I}_M, \end{aligned} \quad (18)$$

where (a) is because of the orthogonality of the DFT matrix, and the (i, j) -th element of Ω is given as

$$[\Omega]_{i,j} = \begin{cases} N\beta_{cas} |x_{\tau_i}|^2 + \sigma_u^2, & i = j, \\ 0, & i \neq j. \end{cases} \quad (19)$$

For simplicity, we let $|x_{\tau_i}|^2 = 1$. Then, plugging (17) and (18) into (16), we get the MMSE estimator given as

$$\begin{aligned} \hat{\mathbf{h}}_t & = ((\beta_{cas} \Phi^H \tilde{\mathbf{D}}) \otimes \mathbf{I}_M) (\Omega \otimes \mathbf{I}_M)^{-1} \psi \\ & = ((\beta_{cas} \Phi^H \tilde{\mathbf{D}}) \otimes \mathbf{I}_M) (\Omega^{-1} \otimes \mathbf{I}_M) \psi \\ & = \frac{\beta_{cas}}{N\beta_{cas} + \sigma_u^2} \left((\Phi^H \tilde{\mathbf{D}}) \otimes \mathbf{I}_M \right) \psi. \end{aligned} \quad (20)$$

Moreover, the covariance matrix of the channel estimate is given as

$$\begin{aligned} \Psi_t & = \mathbb{E} \left[\hat{\mathbf{h}}_t \hat{\mathbf{h}}_t^H \right] \\ & = \mathbb{E} \left[\tilde{\mathbf{h}}_t \psi^H \right] \left(\mathbb{E} [\psi \psi^H] \right)^{-1} \left(\mathbb{E} [\tilde{\mathbf{h}}_t \psi^H] \right)^H \\ & = \beta_{cas}^2 \left((\Phi^H \tilde{\mathbf{D}} \Omega^{-1}) \otimes \mathbf{I}_M \right) \left((\tilde{\mathbf{D}}^H \Phi) \otimes \mathbf{I}_M \right) \\ & = \frac{\beta_{cas}^2}{N\beta_{cas} + \sigma_u^2} \left(\Phi^H \tilde{\mathbf{D}} \tilde{\mathbf{D}}^H \Phi \right) \otimes \mathbf{I}_M. \end{aligned} \quad (21)$$

The corresponding estimation error covariance is given as

$$\begin{aligned} \mathbf{C}_t & = \mathbb{E} [\Delta \mathbf{h}_t \Delta \mathbf{h}_t^H] \\ & = \mathbb{E} \left[\tilde{\mathbf{h}}_t \tilde{\mathbf{h}}_t^H \right] - \mathbb{E} \left[\hat{\mathbf{h}}_t \hat{\mathbf{h}}_t^H \right] \\ & = \beta_{cas} \mathbf{I}_{MN} - \frac{\beta_{cas}^2}{N\beta_{cas} + \sigma_u^2} \left(\Phi^H \tilde{\mathbf{D}} \tilde{\mathbf{D}}^H \Phi \right) \otimes \mathbf{I}_M. \end{aligned} \quad (22)$$

B. Proof of Theorem 1

Based on (10) and (11) the averaged SNR is given as

$$\begin{aligned} \mathbb{E} [\hat{\gamma}_t] & = \frac{P}{\sigma_d^2} \mathbb{E} \left[\left| \left(\mathbf{D}_t \tilde{\mathbf{H}}_{cas} \phi_t^{dl} \right)^T \mathbf{w}_t \right|^2 \right] \\ & = \frac{P}{\sigma_d^2} \left(\mathbb{E} \left[\left\| \hat{\mathbf{H}}_{cas,t} \phi_t^{dl} \right\|^2 \right] \right)^{-1} \\ & \quad \mathbb{E} \left[\left| \left(\tilde{\mathbf{H}}_{cas,t} \phi_t^{dl} \right)^T \left(\hat{\mathbf{H}}_{cas,t} \phi_t^{dl} \right)^* \right|^2 \right], \end{aligned} \quad (23)$$

where the first term of (23) for random IRS is simplified as

$$\begin{aligned} & \mathbb{E} \left[\left\| \hat{\mathbf{H}}_{cas,t} \phi_t^{dl} \right\|^2 \right] \\ & = \mathbb{E} \left[\left\| \left((\phi_t^{dl})^T \otimes \mathbf{I}_M \right) \hat{\mathbf{h}}_t \right\|^2 \right] = \mathbb{E} \left[\left\| \hat{\mathbf{h}}_t \right\|^2 \right] \\ & \stackrel{(a)}{=} \frac{MN(\beta_{cas})^2}{N\beta_{cas} + \sigma_u^2} \sum_{i=1}^N e^{-(\sigma_{BS}^2 + \sigma_{UE}^2) |t-i|} \\ & \stackrel{(b)}{=} MN\eta, \end{aligned} \quad (24)$$

where (a) follows computing $\text{tr}(\Psi_t)$, and (b) is by introducing $\eta = \frac{(\beta_{cas})^2}{N\beta_{cas} + \sigma_u^2} \sum_{i=1}^N e^{-(\sigma_{BS}^2 + \sigma_{UE}^2) |t-i|}$ for readability. Next, we derive $\mathbb{E} \left[\left\| \hat{\mathbf{H}}_{cas,t} \phi_t^{dl} \right\|^2 \right]$ for optimized IRS. By simulations we find that averaged SNR with optimized IRS according (12) is the same with $\phi_{t,opt}^{DL} = \exp \left(j \angle \left(\hat{\mathbf{h}}_{cas,t}^H \right) \right)$, where $\hat{\mathbf{h}}_{cas,t}$ denotes any row of $\tilde{\mathbf{H}}_{cas,t}$. This is also observed in [1]. Therefore, we derive the average SNR with optimized IRS according to $\phi_{t,opt}^{DL} = \exp \left(j \angle \left(\hat{\mathbf{h}}_{cas,t}^H \right) \right)$ in the following.

We use $\hat{\mathbf{H}}'_{cas,t}$ to denote a $(M-1) \times N$ submatrix of $\hat{\mathbf{H}}_{cas,t}$ except for the row $\hat{\mathbf{h}}_{cas,t}$, then we have

$$\begin{aligned}
& \mathbb{E} \left[\left\| \hat{\mathbf{H}}_{cas,t} \phi_{t,opt}^{dl} \right\|^2 \right] \\
& \stackrel{(a)}{=} \mathbb{E} \left[\left\| \hat{\mathbf{h}}_{cas,t} \phi_{t,opt} \right\|^2 + \left\| \hat{\mathbf{H}}'_{cas,t} \phi_{t,opt} \right\|^2 \right] \\
& = \mathbb{E} \left[\left(\sum_{n=1}^N \left| \hat{\mathbf{h}}_{cas,t}(n) \right| \right)^2 \right] + \mathbb{E} \left[\left\| \hat{\mathbf{H}}'_{cas,t} \phi_{t,opt} \right\|^2 \right] \\
& \stackrel{(b)}{=} N^2 \frac{\pi\eta}{4} + (M-1)N\eta, \tag{25}
\end{aligned}$$

where (a) is exploiting the property of the vector norm, and the first term of (b) is because $\hat{\mathbf{h}}_{cas,t}(n)$ follows Rayleigh distribution. While the second term of (b) is derived following same approach as used in (24), since $\phi_{t,opt}$ is only related to $\hat{\mathbf{h}}_{cas,t}$, it can be considered as a random vector in $\mathbb{E} \left[\left\| \hat{\mathbf{H}}'_{cas,t} \phi_{t,opt} \right\|^2 \right]$. Then, the last term of (23) with random IRS is obtained as

$$\begin{aligned}
& \mathbb{E} \left[\left| \left(\tilde{\mathbf{H}}_{cas,t} \phi_t^{dl} \right)^T \left(\hat{\mathbf{H}}_{cas,t} \phi_t^{dl} \right)^* \right|^2 \right] \\
& = \mathbb{E} \left[\left| \left(\left(\hat{\mathbf{H}}_{cas,t} + \Delta \mathbf{H}_{cas,t} \right) \phi_t \right)^T \left(\hat{\mathbf{H}}_{cas,t} \phi_t \right)^* \right|^2 \right] \\
& = \mathbb{E} \left[\left| \left(\hat{\mathbf{H}}_{cas,t} \phi_t \right)^T \left(\hat{\mathbf{H}}_{cas,t} \phi_t \right)^* \right|^2 \right] \\
& \quad + \mathbb{E} \left[\left| \left(\Delta \mathbf{H}_{cas,t} \phi_t \right)^T \left(\hat{\mathbf{H}}_{cas,t} \phi_t \right)^* \right|^2 \right] \\
& = (MN\eta)^2 + MN^2\beta_{cas}\eta - M(N\eta)^2, \tag{26}
\end{aligned}$$

where the last equality follows from algebraic computation of the two independent variables. Similarly, for optimized IRS we have

$$\begin{aligned}
& \mathbb{E} \left[\left| \left(\tilde{\mathbf{H}}_{cas,t} \phi_{t,opt} \right)^T \left(\hat{\mathbf{H}}_{cas,t} \phi_{t,opt} \right)^* \right|^2 \right] \\
& = \left(N^2 \frac{\pi\eta}{4} + (M-1)N\eta \right)^2 \\
& \quad + \text{tr} \left(N(\beta_1\beta_2 - \eta) \text{diag} \left(\left[\frac{N^2\pi}{4}\eta, N\eta, \dots, N\eta \right] \right) \right) \\
& = \left(N^2 \frac{\pi\eta}{4} + (M-1)N\eta \right)^2 \\
& \quad + N(\beta_1\beta_2 - \eta) \left(\frac{N^2\pi}{4}\eta + (M-1)N\eta \right). \tag{27}
\end{aligned}$$

Finally, by plugging (24) (26) into (23), and (25) (27) into (23) we observe theorem 1.

C. Proof of $\Delta\eta \geq 0$

We observe the distance of η between N and $N-1$ as

$$\begin{aligned}
\Delta\eta & = \frac{\beta_{cas}}{N} \sum_{i=1}^N e^{-(\sigma_{BS}^2 + \sigma_{UE}^2)(t-i)} \\
& \quad - \frac{\beta_{cas}}{N-1} \sum_{i=1}^{N-1} e^{-(\sigma_{BS}^2 + \sigma_{UE}^2)(t-i)} \\
& \geq \frac{\beta_{cas} e^{-(\sigma_{BS}^2 + \sigma_{UE}^2)t}}{N(N-1)} \left((N-1)e^{(\sigma_{BS}^2 + \sigma_{UE}^2)N} - (N-1)e^{(\sigma_{BS}^2 + \sigma_{UE}^2)(N-1)} \right) \geq 0,
\end{aligned}$$

where the equality holds when $\sigma_{BS}^2 = \sigma_{UE}^2 = 0$. Thus, η is increasing with N .

REFERENCES

- [1] Q. Wu and R. Zhang, "Intelligent Reflecting Surface Enhanced Wireless Network via Joint Active and Passive Beamforming," *IEEE Transactions on Wireless Communications*, vol. 18, no. 11, pp. 5394–5409, Nov. 2019.
- [2] E. Björnson, Ö. Özdogan, and E. G. Larsson, "Intelligent Reflecting Surface Versus Decode-and-Forward: How Large Surfaces are Needed to Beat Relaying?," *IEEE Wireless Communications Letters*, vol. 9, no. 2, pp. 244–248, Feb. 2020.
- [3] A. Chaaban and A. Sezgin, "Multi-Hop Relaying: An End-to-End Delay Analysis," *IEEE Transactions on Wireless Communications*, vol. 15, no. 4, pp. 2552–2561, 2016.
- [4] T. L. Jensen and E. De Carvalho, "An Optimal Channel Estimation Scheme for Intelligent Reflecting Surfaces Based on a Minimum Variance Unbiased Estimator," in *IEEE International Conference on Acoustics, Speech and Signal Processing (ICASSP)*, May 2020, pp. 5000–5004.
- [5] Q. U. A. Nadeem, H. Alwazani, A. Kammoun, A. Chaaban, M. Debbah, and M. S. Alouini, "Intelligent Reflecting Surface-Assisted Multi-User MISO Communication: Channel Estimation and Beamforming Design," *IEEE Open Journal of the Communications Society*, vol. 1, pp. 661–680, May 2020.
- [6] D. Zito M. Voicu, D. Pepe, "Performance and trends in millimetre-wave CMOS oscillators for emerging wireless applications," *International Journal of Microwave Science and Technology*, 2013.
- [7] A. A. Boulgeorgos E. N. Papisotiriou and A. Alexiou, "Performance Analysis of THz Wireless Systems in the Presence of Antenna Misalignment and Phase Noise," *IEEE Communications Letters*, vol. 24, no. 6, pp. 1211–1215, Jun. 2020.
- [8] P. Hillger, M. van Delden, U. S. M. Thantrige, A. M. Ahmed, J. Witteimer, K. Arzi, et al., "Toward mobile integrated electronic systems at THz frequencies," *Journal of Infrared, Millimeter, and Terahertz Waves*, vol. 41, no. 7, pp. 846–869, 2020.
- [9] A. Papazafeiropoulos, C. Pan, A. Elbir, V. Nguyen, P. Kourtessis, and S. Chatzinotas, "Asymptotic analysis of max-min weighted sinr for irts-assisted miso systems with hardware impairments," *IEEE Wireless Communications Letters*, pp. 1–1, 2021.
- [10] L. Tomba, "On the effect of Wiener phase noise in OFDM systems," *IEEE Transactions on Communications*, vol. 46, no. 5, pp. 580–583, May 1998.
- [11] T. Schenk, *RF imperfections in high-rate wireless systems: impact and digital compensation*, Springer Science & Business Media, 2008.
- [12] E. Basar, M. Di Renzo, J. De Rosny, M. Debbah, M. Alouini, and R. Zhang, "Wireless communications through reconfigurable intelligent surfaces," *IEEE access*, vol. 7, pp. 116753–116773, 2019.
- [13] D. Mishra and H. Johansson, "Channel Estimation and Low-complexity Beamforming Design for Passive Intelligent Surface Assisted MISO Wireless Energy Transfer," in *IEEE International Conference on Acoustics, Speech and Signal Processing (ICASSP)*, May 2019, pp. 4659–4663.
- [14] S. M. Kay, *Fundamentals of statistical signal processing*, Prentice-Hall signal processing series. Prentice Hall PTR, Upper Saddle River, NJ, 1993.